

An investigation of the influence of splitter plates on the vortical wake behind a circular cylinder in cross-flow

Bruno G. Chierigatti, bruno.chierigatti@poli.usp.br

Douglas Serson, douglas.serson@poli.usp.br

Ernani V. Volpe, ernvolpe@usp.br

Julio R. Meneghini, jmeneg@usp.br

NDF, Department of Mechanical Engineering, EP, University of São Paulo; Av. Prof Mello Moraes 2231, Cidade Universitária, São Paulo, Brazil, CEP: 05508-970

Abstract. *Widely recognized for its simplicity, the splitter plate is an effective device for drag reduction in bluff bodies. It consists of a flat plate, which is placed in the center line of wake, in stream wise direction, and it works by changing the way the shear layers interact with one another. The article analyzes the sensitivity the drag force exhibits with respect to the length and position of that simple device. The main purpose is to find out values of those dimensions that lead to a minimum of the time-averaged drag coefficient. The results confirm the literature, to the effect that the extrema depend on the Reynolds number. Moreover, they show that minimum drag configurations may also be characterized by expressive reductions in the amplitude of drag and lift oscillations.*

Keywords: oil risers, splitter plate, drag reduction, optimization

1. INTRODUCTION

Long flexible risers are an essential component of drilling derricks in deep water oil extraction. Their usually bluff cross-sections lead to extensive regions of separated flow. As a result, they shed vortical wakes and are prone to vortex induced vibrations, at all but the lowest Reynolds numbers. Add to it the fact that far-field flow conditions are ultimately determined by the swell and ocean tides, thereby remaining beyond any possibility of control.

Under such circumstances, a deep understanding of the physics of this class of flows is clearly of utmost importance to the oil industry. It has made it a most prolific research topic. Much attention has also been devoted to means of controlling bluff body flows. The possibilities range from active measures, such as forced oscillations [Meneghini, 1993, Meneghini and Bearman, 1995, Meneghini, 2002, Bearman and Currie, 1979, Feng, 1968], to passive devices such as trip-wires, vortex generators and splitter-plates.

Its easy assembly and operation gives the splitter plate an important advantage over many other flow control devices. In principle, it works by extending the length over which the shear layers on each side of a cylinder are separated. It delays the interaction between them, which has the effect of reducing the form drag significantly. In a seminal article on the problem, Igarashi [Igarashi, 1982] classifies the splitter plates according to the way they are assembled, relative to the cylinder. There are configurations where it is attached to the cylinder, and others where there is a gap between the two.

The contribution of the present work is to investigate both cases, with and without gap, in a systematic attempt at finding configurations that yield minimum form drag. The exploratory tests have been performed by means of numerical flow simulations, only. Incidentally, it may be useful to settle on the definitions of the dimensionless parameters early on. The Reynolds (Re) and Strouhal (St) numbers, the pressure (C_p), lift (C_l) and drag (C_d) coefficients are defined as, respectively,

$$\left\{ \begin{array}{l} Re = \frac{U_\infty L}{\nu} \\ St = \frac{fL}{U} \\ q_\infty = \frac{1}{2}\rho_\infty U_\infty^2 \end{array} \right. \quad \left\{ \begin{array}{l} C_p = \frac{p-p_\infty}{q_\infty} \\ C_l = \frac{\|l\|}{q_\infty L} \\ C_d = \frac{\|d\|}{q_\infty L} \end{array} \right. \quad (1)$$

For the sake of completeness: ν is the fluid kinematic viscosity, ρ_∞ and U_∞ are free-stream density and velocity, respectively. The symbol f represents a frequency, which is taken here to be the vortex shedding frequency, U is another velocity scale, which is often taken to be U_∞ , itself, and L is a length scale that depends on the context.

2. LITERATURE SURVEY

For all their relevance in nature and engineering, separated flows are the object of extensive research and a prolific literature, in the realm of fluid mechanics. An inherent complexity has favored the experimental approach in the early years. More recently, though, the development of robust methods of numerical simulation has given rise to an ever-growing field in CFD that is entirely devoted to the topic. This survey attempts to follow the chronology.

In two of the earlier studies on the topic, Roshko has made a semi-empirical analysis of the flow around bluff bodies

[Roshko, 1954a, Roshko, 1954b]. The reports did include cylinders with splitter plates, with and without gaps between them ($Re = 1.45 \times 10^4$). Amongst their most relevant findings, the first one shows that the splitter plate changes the C_p distribution all over the cylinder surface, as opposed to affecting only the separated region. Whereas the second one shows that the dimensionless frequency of vortex shedding (St) decreases as the gap grows, up until a critical value is reached. Then the St jumps back up to a value that is close to that of the isolated cylinder. The cylinder base pressure (C_{pb}) exhibits a similar behavior, with the only difference that it grows a bit, just before the gap reaches the critical value, only to decrease afterwards. The critical size of the gap is identified as the point where the vortex formation region moves from the trailing edge of the plate to the gap, itself.

From 1965, an experimental study on bodies with blunt trailing edges and splitter plates [Bearman, 1965] presents results for C_{pb} , St and velocity fluctuations in the wake, for Re in the range: $1.4 \times 10^5 \leq Re \leq 2.56 \times 10^5$. Among many important results, he has found that the value of $-C_{pb}$ is inversely proportional to the so-called *vortex formation length* (l_f)— which was then defined as the x coordinate of the closest point on the wake axis, where the rms^1 of velocity fluctuations peaks.

A paper by Gerrard [Gerrard, 1966] investigated the physics of the vortex formation region behind bluff bodies. He suggested the key mechanism in vortex formation to be the mutual-interaction between the two shear layers, which arise from boundary layer separation on each side of the cylinder. Furthermore, he proposed that vortex shedding takes place because of fluid entrainment from one layer into the other, in a scheme that is best depicted by his classic sketch— which we took the liberty of reproducing below (fig. 1–left), for clarity.

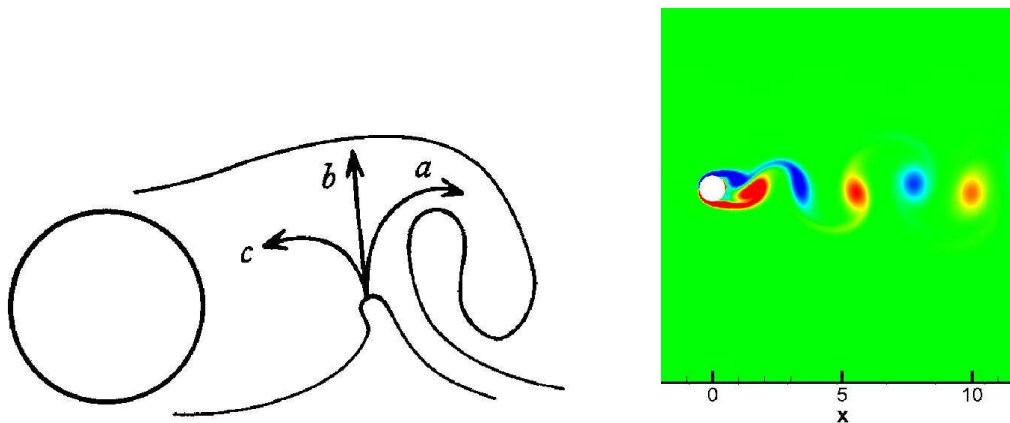


Figure 1. Left, the mechanism of vortex formation behind a circular cylinder, in an excerpt from Gerrard [Gerrard, 1966]. Rolling-up of the shear layers is indicated by filament lines, and the arrows show the fluid path. Right, a numerical simulation of the same problem, which effectively shows the vortex wake behind the cylinder ($Re = 200$).

As is well-known, the fluid on each shear layer bears vorticity of opposite sign. Under this condition, the filament lines show the shear layers rolling up and the arrows indicate the fluid path afterwards. Part of it is entrained by the growing vortex (a). Another part (b) is entrained by the upper shear layer and, on bearing opposite vorticity, it helps to cut the forming vortex off. A third part (c) flows toward the formation region, where it feeds into the lower vortex formation. The formation length l_f is defined here as the point at which the fluid from outside the wake first crosses its axis.

In [Gerrard, 1966], the author performed experiments on cylinders with splitter plates, with and without gaps, and has also reproduced some of Roshko experiments ($Re = 2 \times 10^4$). On doing so, he was able to verify and explain some of Roshko's claims, such as the discontinuity in St that happens as l_f moves from the plate trailing edge to within the gap.

In [Apelt et al., 1973], the authors run a set of experiments involving splitter plates fixed to the basis of the cylinder, for Re in the range: $10^4 \leq Re \leq 5 \times 10^4$. The length $l/d = 1$ was set as a limit, to differentiate between long and short splitter plates. They found that short plates diminish the width of the wake, and stabilize the boundary layer separation points on the cylinder, thus causing the vortices to form closer to the plate trailing edge. Whereas long plates inhibit the interaction between shear layers, thus causing vortices to form farther away from the plate. A sequence to their research was published in [Apelt et al., 1975].

A paper by Igarashi, from 1982 [Igarashi, 1982], reports on extensive experimental research into cylinders with splitter plates. The sizes of the plates and gaps varies within the ranges $0.29 \leq l/d \leq 1.76$ and $0 \leq g/d \leq 4$, respectively. While the Reynolds number is kept within the interval: $1.3 \times 10^4 \leq Re \leq 5.8 \times 10^4$. The results show the variations of shedding frequency (St), base pressure (C_{pb}) and drag (C_d) with respect to gap and plate sizes. Special emphasis is placed upon the discontinuity that happens as the vortex formation moves from the plate trailing edge to within the gap, itself. He also classifies previous works on the topic into three groups, according to their motivations. A first group

¹acronym for root mean square

is primarily concerned with the universal dimensionless frequencies (St) of vortex shedding [Roshko, 1954a, Roshko, 1954b, Gerrard, 1966]. A second group is concerned with the way the plate affects the flow field and, hence, with its effects on lift and drag [Bearman, 1965, Apelt et al., 1973, Apelt et al., 1975]. Finally, a third group focuses on the heat transfer characteristics of the turbulent separated flow region behind the cylinder, as is the case of a later work of his [Igarashi, 1984].

Two articles by Unal and Rockwell on the topic were published in 1988 [Unal and Rockwell, 1988a, Unal and Rockwell, 1988b]. The first one explores the hydrodynamic instabilities that appear in the flow around a cylinder at lower Reynolds ($440 \leq Re \leq 5040$). Whereas the second one analyzes the case of a very long splitter plate, $L/D = 24$, at various gaps, $0 \leq g/d \leq 15$. With regard to the frequencies of velocity fluctuations in the wake, their results have been interpreted as indicative of the thesis that the splitter plate inhibits the vortex shedding, but it does not inhibit the shear layers instability.

In [Kawai, 1990], the author performed numerical simulations of cylinders with splitter plates of various lengths and gaps. He made use of the discrete vortex method, and his results exhibit the same characteristics as those from Roshko and Apelt. Only, his numerical values are different—in particular, the critical gap is about half of the corresponding experimental value. However, the differences have been attributed to differences in the Reynolds number that had been prescribed for the simulations.

A more recent paper by Kwon and Choi [Kwon and Choi, 1996], presents numerical simulations at lower Reynolds numbers ($80 \leq Re \leq 160$). They only considered cases where the splitter plate is fastened to the cylinder. The paper analyzes the behavior of the Strouhal number (St) with changing Re and different plate lengths. Their results are similar to those obtained by Gerrard and Apelt, despite the fact that their simulations have been run at much lower Reynolds numbers.

From the same year, a paper by Nakamura [Nakamura, 1996] analyzes the vortex shedding mechanism for various kinds of bluff bodies, all with splitter plates fastened to their bases. To that end, the author has run experiments for Re between 300 and 500, and has made use of long plates. The paper reports on a gradual transition between two distinct modes of vortex shedding, as the plate length grows. The transition is from the usual mode, which involves mutual interaction between the shear layers, and a mode that is governed by the so-called impinging–shear–layer instability.

It is worth noting that, in all of the above references, the splitter plate has been placed on the axis of the wake. It lies in the same direction of the incoming flow. In effect, whenever that alignment fails, flow and vortex shedding alike change drastically. As a result, it degenerates the device performance as a means of reducing drag. That is indeed one of the major drawbacks of the device. Fortunately, there is a way to circumvent it. For the splitter plate may be hinged on the cylinder, so as to be able to align itself with the incoming flow. Two recent works delve into the subject [Assi et al., 2009, Shukla et al., 2009].

3. RESULTS

The idea that the drag decreases for certain arrangements of the splitter plate is fully consistent with most of the above references. As has been verified by experiment, it happens because the plate can extend the formation length of the wake, depending on its size and position relative to the cylinder. In principle, if there is no gap between cylinder and plate, one could attempt to enhance the effect by increasing the length of the latter. It is clear, though, that the penalty of a growing viscous drag on the plate would eventually offset the benefit. In essence, then, the gap is an attempt at heaping up the benefits of an increased formation length, without incurring the penalty of higher friction drag on the plate.

On the other hand, most references point out that, as the gap exceeds a critical value, which corresponds to minimum drag, the vortex formation region moves within it—it gets enclosed between cylinder and plate. That, in turn, causes the drag to increase abruptly, which thus limits the benefits of this particular device.

One of the references that is directly related to our objectives, [Igarashi, 1982] presents a large collection of experimental results for the flow around cylinders with splitter plates. On following in that author's footsteps, a series of numerical experiments have been performed. The idea was to reproduce his experiments to some extent, if not completely, and to ascertain how much of the flow physics could be captured by the simulations.

Owing to limitations of the numerical method, the values of Re were set in a range lower than his: $100 \leq Re \leq 300$. Various lengths of splitter plate (l) relative to the cylinder diameter (d) were set in the range: $0.5 \leq (l/d) \leq 1.5$. Whereas the relative size of the gap (g/d), ranged from 0 to 4, where g measures the distance from the base of the cylinder to the leading edge of the splitter plate.

All simulations have been performed with the software NEKTAR, which is based on the spectral element method, with Galerkin weighed residuals. The tests have made use of polynomials of 7th order for base functions, and a 2nd order scheme for time stepping. The mesh had 416 elements, with origin at the center of the cylinder. It extended from $-55 \times d$ to $52 \times d$ in the stream-wise direction (x coordinate), and from $-60 \times d$ to $60 \times d$ in the normal direction (y coordinate). These arrangements were defined on the basis of a recent report [Serson and Meneghini, 2010], in which the authors had run a thorough investigation on grid-independence and simulation accuracy, with the same code and for the same class of flows.

No-slip boundary conditions have been imposed on the cylinder wall, while the splitter plate was only imposed the condition $\mathbf{u} \cdot \mathbf{n} = 0$. Hence, the tests do not account for viscous stresses on the plate, nor do they consider the viscous drag thereof. Although the forces on the cylinder are fully accounted for. The set-up is fairly general practice in the CFD community, regarding this class of flows. For it allows a very significant reduction in computational costs. However, it does make for an important difference between numerical and experimental results.

For the purpose of comparison, for each case with a splitter plate, a corresponding test was run without it, under the same flow conditions. As an example, figure 1–right, shows contours of vorticity of the flow around a cylinder without splitter plate, at $Re = 200$. As an illustration of the effects the splitter plate has on the flow, fig. 2 presents vorticity contours for different lengths of splitter plates, all with zero gap ($g/d = 0$). It shows that the wake formation length (l_f) grows with the plate length.

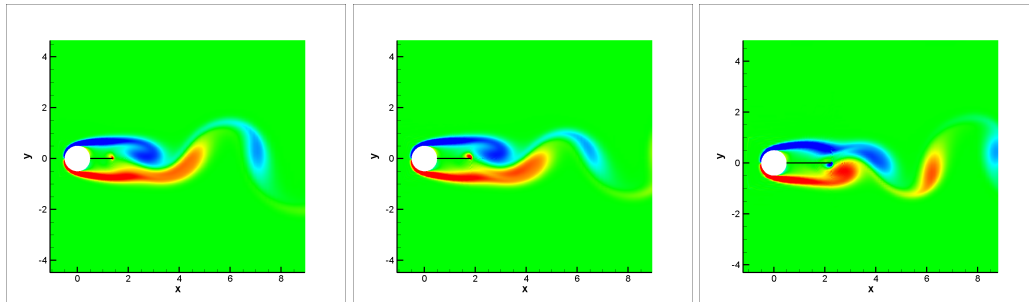


Figure 2. Contours of vorticity of the flow around a cylinder with splitter plate. 2–D flow solutions for different lengths l/d , all of them with no gap between plate and cylinder, at $Re = 200$. From left to right: 1st, $l/d = 0.88$; 2nd, $l/d = 1.32$; 3rd, $l/d = 1.76$.

The effects of the gap are depicted in fig. 3. It presents a sequence of tests where the plate length has been kept constant at $l/d = 0.88$, while the gap was increased from 1.12 to 2.62. The first and second pictures, from left to right, show similar behavior to the zero gap case, in that l_f grows with the spacing between the basis of the cylinder and the plate trailing edge, $(g + l)/d$. Quite a different result is seen in third picture, though. There the gap has grown larger than the formation region, which now lies within it.

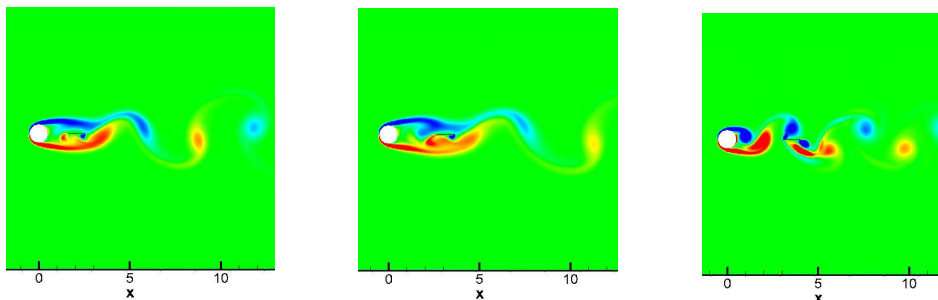


Figure 3. Contours of vorticity of the flow around a cylinder with splitter plate. 2–D flow solutions for different gaps g/d , all of them with the same length $l/d = 0.88$, at $Re = 200$. From top to bottom, left to right: 1st, $g/d = 1.12$; 2nd, $g/d = 2.22$; 3rd, $g/d = 2.62$.

The above changes in the wake structure clearly affect drag and lift forces alike. The unsteady nature of the flow imparts oscillations to the forces— where the latter must have zero mean, owing to flow symmetry. Figure 4 illustrates these effects in time domain, for the case where $l/d = 1$, while g/d is increased from 0.25 to 3, all at $Re = 200$.

In fig. 4–left, it is clear that C_l oscillates with zero mean, as was expected. Furthermore, one sees that not only does the amplitude decrease as the gap grows, but so does the frequency. The trends persist up to a critical point, which represents a minimum for both amplitude and frequency. If the gap grows beyond that point, then both parameters jump back to the same orders of magnitude they exhibit for an isolated cylinder. The same trends can be noticed in fig. 4–right, which shows the C_d evolution. Only, in this case, time averages are clearly nonzero, and one realizes the mean C_d also reaches a minimum at the same critical value of g/d , beyond which it experiences large growth.

In an attempt to give a more systematic view of the results, for different values of Re , l/d and g/d , we picked parameters that should be representative of the periodic flow. To that end, the drag coefficient has been time-averaged over 10 periods of regular oscillations ($\overline{C_d}$). While the lift coefficient evolution is represented by the maximum amplitude

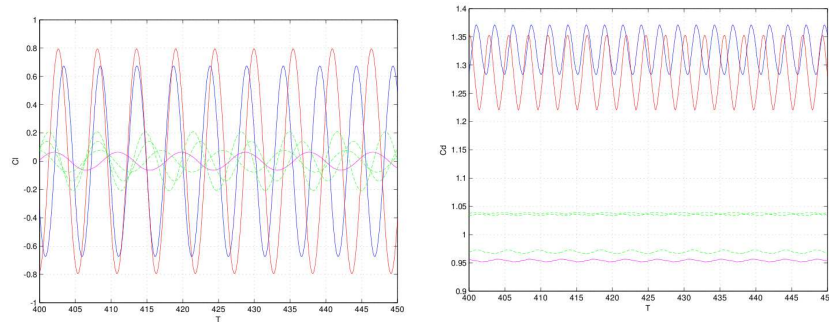


Figure 4. Time dependence of c_l (left) and c_d (right) for different g/d , at $Re = 200$, $l/d = 1.0$. Blue solid line, no splitter plate. Magenta solid line, $g/d = 2.30$, which minimizes the time averaged C_d . Green dash-dot lines, intermediary values of g/d . Red solid line, value of g/d that exceeds formation length, thus allowing shear layers to interact within the gap.

of its oscillations over the same time-span. In addition to that, the Strouhall number (St) and formation length (l_f) are plotted against gap (g/d), as part of the analysis.

Figure 5 compares an isolated cylinder to cylinders with splitter plates, but no gap, with respect to values of $\overline{C_d}$ and C_l maximum amplitude. Various plate lengths are considered. As can be seen, the plate can reduce the time-averaged drag up to 17.5%, while it also diminishes the C_l amplitude by up to 60.6%.

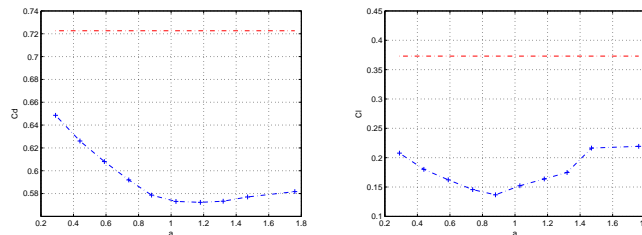


Figure 5. Time-averaged $\overline{C_d}$ and C_l amplitude for the zero gap configuration as functions l/d , at $Re = 200$. Red dash-dot lines, no splitter plate. Blue dash-dot lines, with splitter plate. Left, $\overline{C_d} \times l/d$; right, C_l amplitude $\times l/d$.

As it is pointed out by [Igarashi, 1982], experimental results show the mean drag reaches a minimum at a certain plate length. Beyond that, the value of $\overline{C_d}$ grows back, as a result of an increasing viscous drag on the plate itself, thus offsetting its original benefit. In the above results, $\overline{C_d}$ is shown to level off, instead. As was mentioned above, the behavior is owed to the fact that the viscous drag on the plate has been neglected.

Figures 6–8 bring results for $\overline{C_d}$ and maximum C_l amplitude in a set of tests, for three distinct plate lengths: $l/d = 0.5$, $l/d = 1.0$ and $l/d = 1.5$, respectively; all at $Re = 200$. These tests have focused on the dependence of $\overline{C_d}$ and C_l amplitude on the gap size g/d , for a fixed Re .

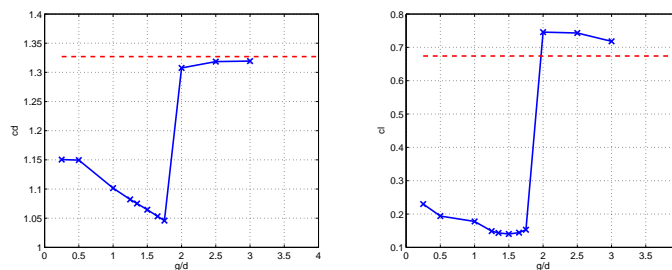


Figure 6. Maximum amplitude of C_l and $\overline{C_d}$ versus g/d , at $Re = 200$ and $l/d = 0.5$. Red dash-dot lines, no splitter plate. Blue dash-dot lines, with splitter plate. Left, $\overline{C_d}$; right, C_l maximum amplitude.

The results show the mean drag can be reduced by up to 20.5% for $l/d = 0.5$, by 28.1% for $l/d = 1.0$ and by 30.4% for $l/d = 1.5$. It is also clear that, in all cases, on increasing the gap just beyond the point of minimum $\overline{C_d}$, that coefficient undergoes a sharp jump discontinuity, thus reaching values that are close to that of the isolated cylinder. The jump is an

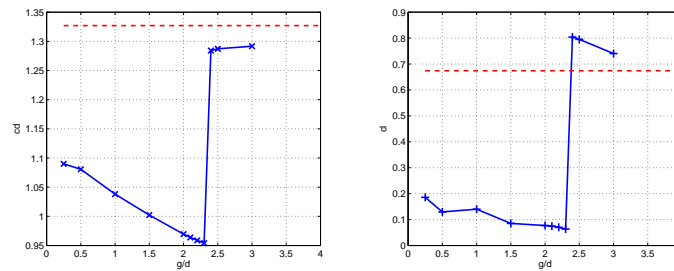


Figure 7. Maximum amplitude of C_l and $\overline{C_d}$ versus g/d , at $Re = 200$ and $l/d = 1.0$. Red dash-dot lines, no splitter plate. Blue dash-dot lines, with splitter plate. Left, $\overline{C_d}$; right, C_l maximum amplitude.

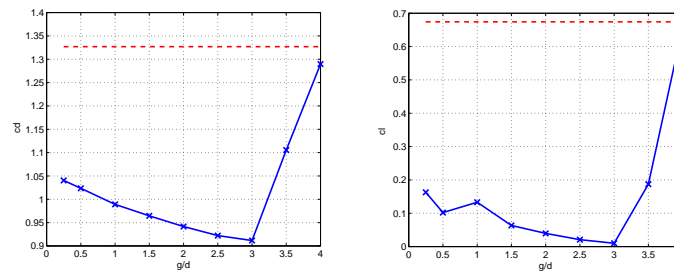


Figure 8. Maximum amplitude of C_l and $\overline{C_d}$ versus g/d , at $Re = 200$ and $l/d = 1.5$. Red dash-dot lines, no splitter plate. Blue dash-dot lines, with splitter plate. Left, $\overline{C_d}$; right, C_l maximum amplitude.

immediate result of the fact the vortex formation region has moved into the gap. As for the maximum amplitude of C_l oscillations, the device reduces it by up to 74.5% in the first case, 87.0% in the second and 92.8% in the third.

It must also be noted that the values of g/d that lead to minimum $\overline{C_d}$ and minimum C_l amplitude for each case are either coincident or very close to it. Moreover, the behavior of the C_l amplitude strongly resembles that of $\overline{C_d}$, in that both grow rapidly beyond their minimum. These features are further evidence that the vortex formation length virtually controls the physics of this class of flows. In that sense, it is noteworthy that the numerical simulations could capture such substantial part of the physics, despite the neglect of viscous stresses on the plate.

The exact same trends are verified for other values of the Reynolds number, such as $Re = 100$ and $Re = 300$. The results are shown in the sets of figures. 9–11 and 12–14, respectively.

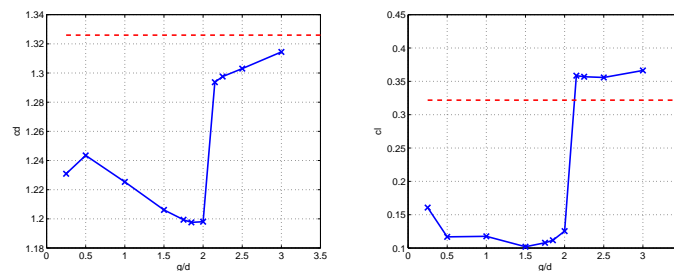


Figure 9. Maximum amplitude of C_l and $\overline{C_d}$ versus g/d , at $Re = 100$ and $l/d = 0.5$. Red dash-dot lines, no splitter plate. Blue dash-dot lines, with splitter plate. Left, $\overline{C_d}$; right, C_l maximum amplitude.

Test results for $Re = 100$ show the $\overline{C_d}$ can be reduced by up to 9.1% for $l/d = 0.5$, by 15.2% for $l/d = 1.0$ and by 16.7% for $l/d = 1.5$, while the maximum amplitude of C_l oscillations decreases by 62.8%, 84.4% and 87.5%, respectively. Although they are a bit smaller than the previous case, the numbers are, nonetheless, of the same order of magnitude.

For the case with $Re = 300$, the reduction in $\overline{C_d}$ is of about 27.5% for $l/d = 0.5$, of 26.9% for $l/d = 1.0$ and of 24.1% for $l/d = 1.5$. While the maximum amplitude of C_l oscillations is diminished by about 77.2%, 83.4% and 88.9%, respectively. Here again, the results are of the same order of magnitude as the previous cases.

On comparing results for the same plate length, at different Reynolds numbers, one notices that the value of g/d for

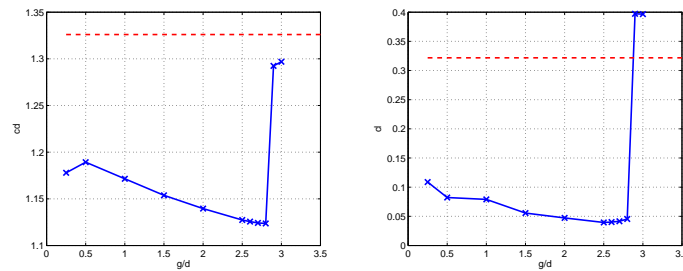


Figure 10. Maximum amplitude of C_l and $\overline{C_d}$ versus g/d , at $Re = 100$ and $l/d = 1.0$. Red dash-dot lines, no splitter plate. Blue dash-dot lines, with splitter plate. Left, $\overline{C_d}$; right, C_l maximum amplitude.

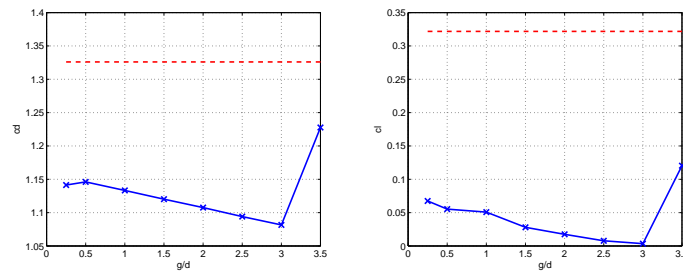


Figure 11. Maximum amplitude of C_l and $\overline{C_d}$ versus g/d , at $Re = 100$ and $l/d = 1.5$. Red dash-dot lines, no splitter plate. Blue dash-dot lines, with splitter plate. Left, $\overline{C_d}$; right, C_l maximum amplitude.

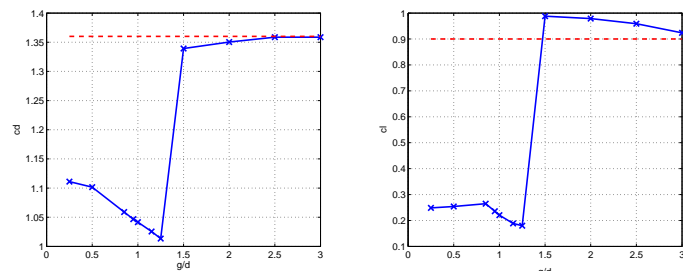


Figure 12. Maximum amplitude of C_l and $\overline{C_d}$ versus g/d , at $Re = 300$ and $l/d = 0.5$. Red dash-dot lines, no splitter plate. Blue dash-dot lines, with splitter plate. Left, $\overline{C_d}$; right, C_l maximum amplitude.

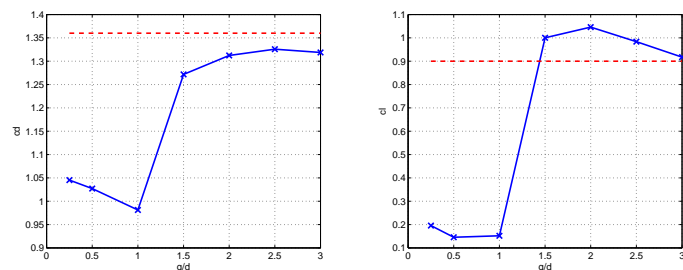


Figure 13. Maximum amplitude of C_l and $\overline{C_d}$ versus g/d , at $Re = 300$ and $l/d = 1.0$. Red dash-dot lines, no splitter plate. Blue dash-dot lines, with splitter plate. Left, $\overline{C_d}$; right, C_l maximum amplitude.

minimum $\overline{C_d}$ diminishes with growing Re . In a sense, the trend is consistent with the case of an isolated cylinder, for which higher values of Re are known to lead to smaller formation lengths [Serson and Meneghini, 2010]. A different picture emerges on comparing gap sizes for different l/d at the same Re . That comparison shows the value of g/d that yields minimum $\overline{C_d}$ grows with the relative length.

The effects of the gap size on the Strouhal number (St), for different Re , at a fixed plate length, $l/d = 0.5$, are

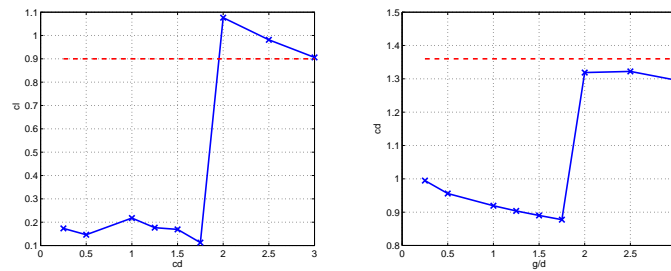


Figure 14. Maximum amplitude of C_l and $\overline{C_d}$ versus g/d , at $Re = 300$ and $l/d = 1.5$. Red dash-dot lines, no splitter plate. Blue dash-dot lines, with splitter plate. Left, $\overline{C_d}$; right, C_l maximum amplitude.

depicted in fig. 15. It must be noted that St has been defined here on the basis of the vortex shedding frequency, free-stream velocity and cylinder diameter. A similar analysis is presented in fig. 16 for the case where $l/d = 1.0$.

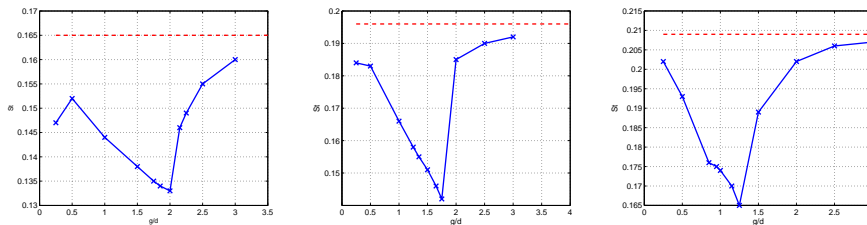


Figure 15. Strouhal number St versus gap size g/d , for $l/d = 0.5$. Left, $Re = 100$; center, $Re = 200$; right, $Re = 300$. Red dash-dot lines, no splitter plate; blue dash-dot lines, with splitter plate.

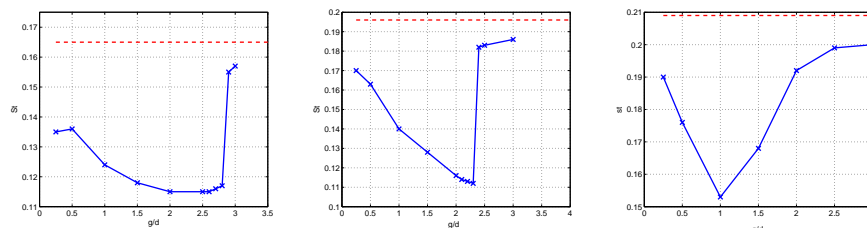


Figure 16. Strouhal number St versus gap size g/d , for $l/d = 1.0$. Left, $Re = 100$; center, $Re = 200$; right, $Re = 300$. Red dash-dot lines, no splitter plate; blue dash-dot lines, with splitter plate.

The same trends are seen in all cases, in that there is a pronounced decrease in St with growing g/d . As the gap is increased beyond the point of minimum, the Strouhal number grows steeply, only to reach values that are closer to that of the isolated cylinder. However, the most remarkable feature of these results lies in the fact that the point of minimum vortex shedding frequency coincides with the point of minimum mean drag $\overline{C_d}$ and minimum amplitude of C_l oscillations.

Figures 17 and 18 show the effects of the gap size on the vortex formation length (l_f), for two sizes of splitter plate: $l/d = 0.5$ and $l/d = 1.0$, respectively. The parameter l_f has been defined here as the x coordinate of the first point on wake axis ($y = 0$) where the time-averaged x component of the flow velocity goes through zero. The figures bring the parameter in dimensionless form, that is: $l_f/d \times g/d$.

The above results corroborate the hypothesis that the formation length controls this class of flows. For they show l_f/d grows with g/d up to a maximum, which corresponds to the minimum values of $\overline{C_d}$, C_l amplitude and St . In the ascent, the flow physics is such that $l_f/d \geq (g + l)/d$. When the gap is increased beyond the point of maximum l_f , it falls to levels that are comparable to that of the isolated cylinder. In essence, that implies the vortex formation region gets contained within the gap, $l_f/d \leq g/d$.

For completeness figs. 19 and 20 present the pressure coefficient at the base of the cylinder versus gap size ($-C_{pb} \times g/d$) for $l/d = 0.5$ and $l/d = 1.0$, respectively. Here, it is understood that C_{pb} is based on a time-average of pressure over a time-span of 10 regular periods, and the base corresponds to the point $(x, y) = (d/2, 0)$, where the origin is at the center of the cylinder and the x axis is oriented downstream.

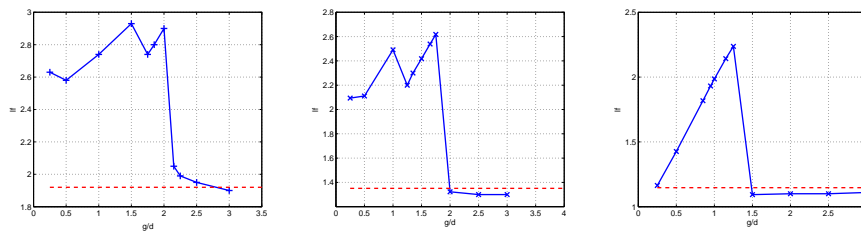


Figure 17. Dimensionless formation length l_f/d versus gap size g/d , for $l/d = 0.5$. Left, $Re = 100$; center, $Re = 200$; right, $Re = 300$. Red dash-dot lines, no splitter plate; blue dash-dot lines, with splitter plate.

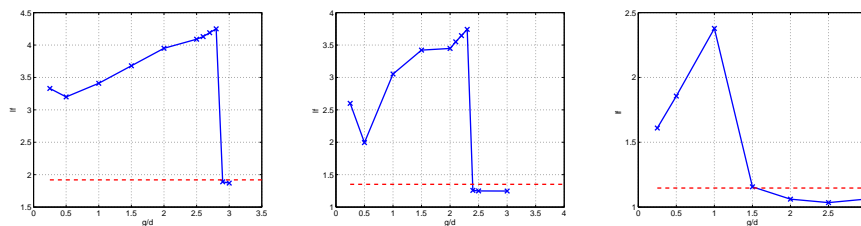


Figure 18. Dimensionless formation length l_f/d versus gap size g/d , for $l/d = 1.0$. Left, $Re = 100$; center, $Re = 200$; right, $Re = 300$. Red dash-dot lines, no splitter plate; blue dash-dot lines, with splitter plate.

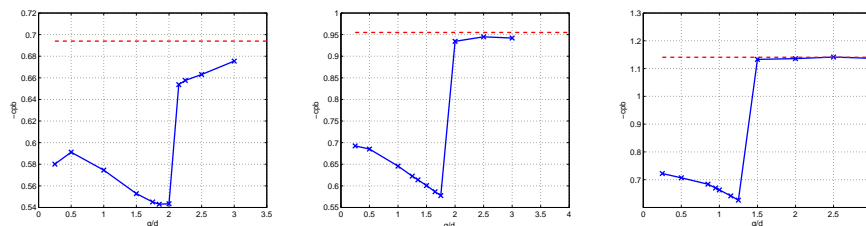


Figure 19. Base Pressure Coefficient $-C_{pb}$ versus gap size g/d , for $l/d = 0.5$. Left, $Re = 100$; center, $Re = 200$; right, $Re = 300$. Red dash-dot lines, no splitter plate; blue dash-dot lines, with splitter plate.

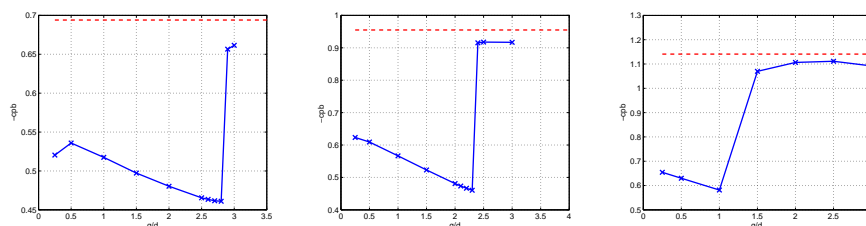


Figure 20. Base Pressure Coefficient $-C_{pb}$ versus gap size g/d , for $l/d = 1.0$. Left, $Re = 100$; center, $Re = 200$; right, $Re = 300$. Red dash-dot lines, no splitter plate; blue dash-dot lines, with splitter plate.

As is widely reported in the literature, $-C_{pb}$ shows strong correlation with the corresponding form drag, $\overline{C_d}$. The results give further evidence of the accuracy of the numerical simulations, which have been performed here.

4. CONCLUDING REMARKS

A systematic investigation has been performed into the flow around a circular cylinder with a wake splitter plate. It has involved a number of numerical simulations, and has considered various plate lengths and gap sizes. The Reynolds number has been set at values within the range $100 \leq Re \leq 300$, and the flow model was substantially simplified, in that viscous stresses on the splitter plate have been neglected.

In spite of the simplification, the results have shown to capture such relevant aspects of the flow physics, as the discontinuity the vortex formation length experiences, as a function of the gap size. That discontinuity is characterized

by a finite jump, which is owed to the transition of the vortex formation region from downstream of the plate to within the gap, itself. The jump is preceded by the maximum formation length, and that same extremum is also associated with minimum values for the time-averaged form-drag, amplitude of lift oscillations, and vortex shedding frequency. Yet, our results suggest its dependence on the Reynolds number may be stronger in this range, than it had been anticipated in previous works.

With regard to potential applications the device has in the oil industry, that extremum truly represents the optimum configuration. However, its dependence on the Reynolds number prompts the need for further analysis, and may entail compromise solutions. After all, that parameter is naturally beyond control in oceanic systems.

5. REFERENCES

- Apelt, C. J., West, G. S., and Szewczyk, A. A., 1973, The effects of wake splitter plates on bluff-body flow in the range $10^4 < R < 5 \times 10^4$, "Journal of Fluid Mechanics", Vol. 61, No. 1, pp. 187–198.
- Apelt, C. J., West, G. S., and Szewczyk, A. A., 1975, The effects of wake splitter plates on bluff-body flow in the range $10^4 < R < 5 \times 10^4$. Part 2., "Journal of Fluid Mechanics", Vol. 71, No. 1, pp. 145–160.
- Assi, G. R., Bearman, P. W., and Kitney, N., 2009, Low drag solutions for suppressing vortex-induced vibration of circular cylinders, "Journal of Fluids and Structures", Vol. 25, No. 4, pp. 666–675.
- Bearman, P. W., 1965, Investigation of the flow behind a two-dimensional model with a blunt trailing edge and fitted with splitter plates, "Journal of Fluid Mechanics", Vol. 21, No. 2, pp. 241–255.
- Bearman, P. W. and Currie, I. G., 1979, Pressure fluctuation measurements on an oscillating circular cylinder, "Journal of Fluid Mechanics", Vol. 91, No. 4, pp. 661–667.
- Feng, C. C., 1968, The measurement of vortex-induced effects in a flow past stationary and oscillating circular and D-section cylinders, M.sc. thesis, University of British Columbia, Canada.
- Gerrard, J., 1966, The mechanics of the formation region of vortices behind bluff bodies, "Journal of Fluid Mechanics", Vol. 25, No. 2, pp. 401–413.
- Igarashi, T., 1982, Investigation on the Flow behind a Circular Cylinder with a Wake Splitter Plate, "Bulletin of the JSME", Vol. 25, No. 202, pp. 528–535.
- Igarashi, T., 1984, Correlation between heat transfer and fluctuating pressure in separated region of a circular cylinder, "International Journal of Heat and Mass Transfer", Vol. 27, No. 6, pp. 927–937.
- Kawai, H., 1990, Discrete vortex simulation for flow around a circular cylinder with a splitter plate, "Journal of Wind Engineering and Industrial Aerodynamics", Vol. 33, No. 1.
- Kwon, K. and Choi, H., 1996, Control of laminar vortex shedding behind a circular cylinder using splitter plates, "Physics of Fluids", Vol. 8, No. 2, pp. 479–486.
- Meneghini, J. R., 1993, "Numerical Simulation of Bluff Body Flow Control Using a Discrete Vortex Method", PhD thesis, Imperial College of Science, Technology and Medicine, University of London, London, UK.
- Meneghini, J. R., 2002, Geração e Desprendimento de Vórtices no Escoamento ao Redor de Cilindros, Tese de livre docência, Escola Politécnica da Universidade de São Paulo, São Paulo.
- Meneghini, J. R. and Bearman, P. W., 1995, Numerical simulation of high amplitude oscillatory flow about a circular cylinder, "Journal of Fluids and Structures", Vol. 9, pp. 435–455.
- Nakamura, Y., 1996, Vortex shedding from bluff bodies with splitter plates, "Journal of Fluid and Structures", Vol. 10, No. 2, pp. 147–158.
- Roshko, A., 1954a, On the development of turbulent wakes from vortex streets, Report 1191, NACA.
- Roshko, A., 1954b, On the drag and shedding frequency of two-dimensional bluff bodies, Technical Note 3169, NACA.
- Serson, D. and Meneghini, J. R., 2010, Simulações Numéricas do Escoamento ao redor de um Cilindro com Splitter Plate, Research Report 1, Escola Politécnica da Universidade de São Paulo, Brazil, Projeto FAPESP 2009/14233–1.
- Shukla, S., Govardhan, R. N., and Arakeri, J. H., 2009, Flow over a cylinder with a hinged-splitter plate, "Journal of Fluids and Structures", Vol. 25, No. 4, pp. 713–720.
- Unal, F. M. and Rockwell, D., 1988a, On vortex formation from a cylinder. Part 1. The initial instability., "Journal of Fluid Mechanics", Vol. 190, pp. 491–512.
- Unal, F. M. and Rockwell, D., 1988b, On vortex formation from a cylinder. Part 2. Control by splitter-plate interference., "Journal of Fluid Mechanics", Vol. 190, pp. 513–529.

6. Responsibility notice

The authors are the only responsible for the printed material included in this paper